Journal of Marine Systems 139 (2014) 311–319

Contents lists available at ScienceDirect

Journal of Marine Systems

journal homepage: www.elsevier.com/locate/jmarsys

# Observed near-surface currents under four super typhoons

Yu-Chia Chang [a,*], Peter C. Chu [b], Luca R. Centurioni [c], Ruo-Shan Tseng [d]

[a] Department of Marine Biotechnology and Resources, National Sun Yat-sen University, Kaohsiung 80424, Taiwan
[b] Naval Ocean Analysis and Prediction Laboratory, Department of Oceanography, Naval Postgraduate School, Monterey, CA 93943, USA
[c] Scripps Institution of Oceanography, La Jolla, CA 92093-0213, USA
[d] Department of Oceanography, National Sun Yat-sen University, Kaohsiung 80424, Taiwan

ARTICLE INFO

*Article history:*
Received 16 January 2014
Received in revised form 12 May 2014
Accepted 10 July 2014
Available online 16 July 2014

*Keywords:*
SVP drifter
Super typhoon
Current velocity
Northwestern Pacific Ocean
Saffir–Simpson hurricane scale

ABSTRACT

The upper ocean currents under four category-5 (super) typhoons [Chaba (2004), Maon (2004), Saomai (2006), and Jangmi (2008)] were studied using data from four drifters of the Surface Velocity Program (SVP) (Niiler, 2001) in the northwestern Pacific. Maximum current velocities occurring to the right of the super typhoon tracks were observed as 2.6 m $s^{-1}$ for slow-moving (2.9 m $s^{-1}$) Maon, 2.1 m $s^{-1}$ for typical-moving Chaba (5.1 m $s^{-1}$), 1.4 m $s^{-1}$ for fast-moving Jangmi (6.8 m $s^{-1}$), and 1.2 m $s^{-1}$ for fast-moving Saomai (8.1 m $s^{-1}$). Furthermore, dependence of the mixed layer current velocity under a super typhoon on its translation speed and statistical relationships between the maximum current speed and the Saffir–Simpson hurricane scale are also provided.

© 2014 Elsevier B.V. All rights reserved.

## 1. Introduction

The characteristics of current velocities in the upper ocean under moving tropical cyclones (TCs) were obtained in many theoretical, observational, and numerical studies. Direct current measurements under TCs during their passages include moored current meters, airborne expendable current profilers (AXCPs), drifting buoys, electromagnetic-autonomous profiling explorer (EM-APEX) floats, Surface Velocity Program (SVP) (Niiler, 2001) drifters, and acoustic Doppler current profilers (ADCPs). Maximum current velocities of 0.3–1.0 m $s^{-1}$ were observed from earlier current meter moorings in the ocean mixed layer (OML) and thermocline as hurricanes passing by within about 60–100 km of these moorings (Brink, 1989; Brooks, 1983; Dickey et al., 1998; Shay and Elsberry, 1987). Strong rightward-biased currents in the upper OML were identified from 0.8 to 1.7 m $s^{-1}$ from AXCPs under tropical storm (TS), category-1, category-3, and category-4 hurricanes (Price et al., 1994; Sanford et al., 1987; Shay and Uhlhorn, 2008), and from 1.0 to 1.5 m $s^{-1}$ from 3 profiling EM-APEX floats under category-4 hurricane Frances 2004 (D'Asaro et al., 2007; Sanford et al., 2011).

Maximum current velocities of 2.0 m $s^{-1}$ and 1.7 m $s^{-1}$ were observed under a category-4 typhoon (Shanshan 2006) and a category-2 typhoon (Haitang 2005) in the Pacific Ocean and the Taiwan Strait (Chang et al., 2010) from the SVP drifter data. Maximum velocities of 0.4–1.6 m $s^{-1}$ in the OML were observed from an ADCP mooring under three fast-moving storms (Black and Dickey, 2008). Maximum velocities of 0.8 m $s^{-1}$ and 0.4 m $s^{-1}$ were also observed from 3 ADCPs inside the radius of wind speeds of 28 m $s^{-1}$ and 18 m $s^{-1}$ during category-5 Hurricanes Katrina and Rita in 2005 (Jaimes and Shay, 2009). However, the ADCPs were located at 4.5 times of the radius of maximum wind ($4.5R_{max}$) for Hurricane Katrina and $17.5R_{max}$ for Hurricane Rita. The strongest currents with a maximum velocity of 2.1 m $s^{-1}$ were measured on the shelf of northeastern Gulf of Mexico in 2004 by an array of 14 ADCPs during category-4 Hurricane Ivan passing through (Mitchell et al., 2005; Teague et al., 2007). The observed maximum current velocities and the storm's track in the earlier studies are listed in Table 1.

In addition to current acceleration, existing modeling studies showed that TCs enhance drastically the upper ocean mixing and in turn affect the fluxes of heat and moisture across the air–ocean interface and change the dynamic height and sea surface temperature with the bias towards the right-side (Chang and Anthes, 1978; Chu et al., 2000; Jacob and Shay, 2003; Olabarrieta et al., 2012; Price, 1981; Price et al., 1994; Warner et al., 2010; Yablonsky and Ginis, 2009; Zambon et al., submitted for publication); and that TCs' passage affects upper ocean responses to the Kuroshio currents in the northwestern Pacific (Kuo et al., 2011; Tsai et al., 2008; Wu et al., 2008).

Two types of oceanic response to a moving TC exist depending on the Froude number, $F_r = U_h/c_1$, with $U_h$ the TC's translation speed, and $c_1$ the phase speed of the first baroclinic mode, which is about 2.8 m $s^{-1}$ in the northwestern Pacific Ocean during summer (Chang et al., 2013). For $F_r > 1$, the response is baroclinic with a wake consisting of the near-inertial waves as the dominant feature. For $F_r < 1$, the oceanic response is barotropic without wake, but with upwelling in the TC's center

* Corresponding author at: 70 Lienhai Rd., Kaohsiung 80424, Taiwan, R.O.C.
*E-mail address:* ycchang@staff.nsysu.edu.tw (Y.-C. Chang).

http://dx.doi.org/10.1016/j.jmarsys.2014.07.011
0924-7963/© 2014 Elsevier B.V. All rights reserved.

**Table 1**
Observed maximum current speeds in earlier studies and corresponding storm track data.

| Storm's name | Hurricane scale | $U_h$ (m s$^{-1}$) | Instrument | Distance (km) | Depth (m) | Reference | $U_{max}$ (m s$^{-1}$) |
|---|---|---|---|---|---|---|---|
| Frederic (1979), Gulf of Mexico | Category-3 | 6.5 | Current meter | 80 | 21 | Shay and Elsberry (1987) | 0.9 |
| Allen (1980), Gulf of Mexico | Category-4 | 3.5 | Current meter | 60 | 200 | Brooks (1983) | 0.9 |
| Norbert (1984), Pacific | Category-1 | 3.2 | AXCP | 89 | 35 | Price et al. (1994) | 1.1 |
| Josephine (1984), Atlantic | Tropical storm | 3.5 | AXCP | 35 | 70 | Price et al. (1994) | 0.8 |
| Gloria (1984), Atlantic | Category-1 | 6.8 | Current meter | 100 | 159 | Brink (1989) | 0.3 |
| Gloria (1985), Atlantic | Category-1 | 6.8 | AXCP | 131 | 55 | Price et al. (1994) | 1.7 |
| Gilbert (1988), Gulf of Mexico | Category-3 | 5.6 | AXCP | 50 | 30 | Shay et al. (1992) | 1.4 |
| Felix (1995), Atlantic | Category-1 | 6.9 | Current meter | 65 | 25 | Dickey et al. (1998) | 1.0 |
| Isidore (2002), Gulf of Mexico | Category 3 | 4.0 | AXCP | * | 60 | Shay and Uhlhorn (2008) | 1.7 |
| Lili (2002), Gulf of Mexico | Category 4 | 7.0 | AXCP | * | 50 | Shay and Uhlhorn (2008) | 1.1 |
| Fabian (2003), Atlantic | Category-3 | 8.6 | ADCP | 102 | 60 | Black and Dickey (2008) | 1.6 |
| Frances (2004), Atlantic | Category-4 | 6.0 | EM-APEX | 55 | 30 | Sanford et al. (2011) | 1.5 |
| Ivan (2004), Gulf of Mexico | Category-4 | 5.8 | ADCP | 15 | 6 | Teague et al. (2007) | 2.1 |
| Harvey (2005), Atlantic | Tropical storm | 6.3 | ADCP | 5 | 18 | Black and Dickey (2008) | 0.4 |
| Nate (2005), Atlantic | Category-1 | 6.7 | ADCP | 123 | 18 | Black and Dickey (2008) | 0.4 |
| Hai-tang (2005), Pacific | Category-2 | 2.6 | SVP drifter | 130 | 15 | Chang et al. (2010) | 1.7 |
| Katrina (2005), Gulf of Mexico | Category-5 | 6.3 | ADCP | 120 | 120 | Jaimes and Shay (2009) | 0.8 |
| Rita (2005), Gulf of Mexico | Category-5 | 4.7 | ADCP | 200 | 100 | Jaimes and Shay (2009) | 0.4 |
| Shanshan (2006), Pacific | Category-4 | 2.6 | SVP drifter | 80 | 15 | Chang et al. (2010) | 2.0 |

(Chang and Anthes, 1978; Geisler, 1970). The initial horizontal scales of TCs' wake depend directly on the scales of the atmospheric forcing (Gill, 1984). The typhoon wind-forcing on the ocean mixed layer (OML) currents is near-resonant on the right side but not on the left side of the track (Price, 1981, 1983; Price et al., 1994). Thus, the OML currents are mainly determined by the wind stress with maximum current speed to the right of the storm track at the distance of 1–2$R_{max}$ (mean $R_{max}$ = 47 km) (Brooks, 1983; Chang et al., 2013; Hsu and Yana, 1998). Questions arise: What are the characteristics of OML currents to the right of the storm track at ~1–2$R_{max}$ under category-5 super typhoons from direct velocity measurements? How high can the observed velocity be under the high wind speed of ~70 m s$^{-1}$? What are the differences of observed currents under the slow-moving, typical-moving, and fast-moving super typhoons? What are the general relationships between the maximum current speeds and the Saffir–Simpson hurricane scale? The goal of this study is to answer these questions. To do so, the SVP drifter data in the northwestern Pacific are used to represent the observed upper ocean currents during four super typhoons.

## 2. Four super typhoons

Chaba, Maon, Saomai, and Jangmi became category-5 (super) typhoons in the northwestern Pacific Ocean on 22 August 2004, 7 October 2004, 9 August 2006, and 27 September 2008, with the minimum sea level pressures of 879, 898, 898, and 918 mbar, respectively. Chaba (2004) had typical translation speeds; Maon (2004) had variable translation speeds; and Saomai (2006) and Jangmi (2008) had fast translation speeds. As their intensities reached category 5, their translation speeds ($U_h$) were 4.1–5.2 m s$^{-1}$, 2.9–15.4 m s$^{-1}$, 7.0–8.7 m s$^{-1}$, and 6.7–6.8 m s$^{-1}$ respectively. The characteristics of the four super typhoons as well as corresponding drifters' information are listed in Table 2.

## 3. TC and current velocity data

Data about the four super typhoons with a temporal resolution of 6 h were acquired from the best-track data from the Joint Typhoon Warning Center (JTWC, http://metocph.nmci.navy.mil/jtwc.php). The SVP drifter has a drogue centered at a depth of 15 m beneath the sea surface to measure OML velocities. The velocity data with a 6-hourly resolution were obtained from the Global Drifter Program (GDP) website (http://www.aoml.noaa.gov/phod/dac/dacdata.php) (Hansen and Poulain, 1996). The estimated accuracy of the velocity measurements is $10^{-2}$ m s$^{-1}$ using SVP drifters in a 10 m s$^{-1}$ wind (Niiler et al., 1995).

The four SVP drifters (Argos ID:39606, 2236911, 54688, and 70324) measured the near-surface current velocities under the four super typhoons [Chaba (2004), Maon (2004), Saomai (2006), and Jangmi (2008)] (see Fig. 1). Figs. 2 and 3 show the drifters' trajectories, observed current vectors, and storms' tracks. The four drifters were all located on the right sides of the four storm tracks as the typhoons passed by.

Chaba (2004) was a typical-moving TC. At 00:00 on 22 August, it was in category-3 with a translation speed of 7.0 m s$^{-1}$ and a distance ($D$) of 140 km between the drifter 39606 and storm center. The observed current velocity ($U_{obs}$) from the drifter was 0.9 m s$^{-1}$. When Chaba reached category-4 intensity at 06:00 on 22 August, its translation speed $U_h$ decreased to 5.5 m s$^{-1}$; and the observed current velocity increased to 1.5 m s$^{-1}$ with $D$ = 59 km. Six hours later, Chaba was identified as a category-5 typhoon, and the translation speed $U_h$ decreased slightly to 5.1 m s$^{-1}$ (Fig. 4). A maximum velocity of 2.1 m s$^{-1}$ was measured with $D$ = 69 km.

Maon (2004) was a slow-moving TC. As the storm gradually approached the drifter 2236911 ($D$ = 278, 201, 135, 73, and 31 km), it still moved slowly with the translation speeds of 3.2–3.6 m s$^{-1}$ within 30 h (Fig. 5). Moan strengthened from a category-1 to category-2 intensity during this period. The observed current velocities gradually

**Table 2**
Characteristics of the four super typhoons (Chaba, Maon, Saomai, and Jangmi).

| Storm's name | Chaba 2004 | Maon 2004 | Saomai 2006 | Jangmi 2008 |
|---|---|---|---|---|
| Time as a super typhoon | 1200 22 Aug–0600 26 Aug | 1800 07 Oct–0000 09 Oct | 0600 09 Aug–0600 10 Aug | 0600 24 Sep–1200 30 Sep |
| Minimum sea level pressure (mbar) | 879 | 898 | 898 | 918 |
| $U_h$ (m s$^{-1}$) as a super typhoon | 4.1–5.2 | 2.9–15.4 | 7.0–8.7 | 6.7–6.8 |
| Drifter's ID | 39606 | 2236911 | 54688 | 70324 |
| Date as the distance $D$ < 400 km | 1800 21 Aug–1200 23 Aug | 1200 05 Oct–1200 08 Oct | 0000 09 Aug–0000 10 Aug | 1800 26 Sep–0600 28 Sep |

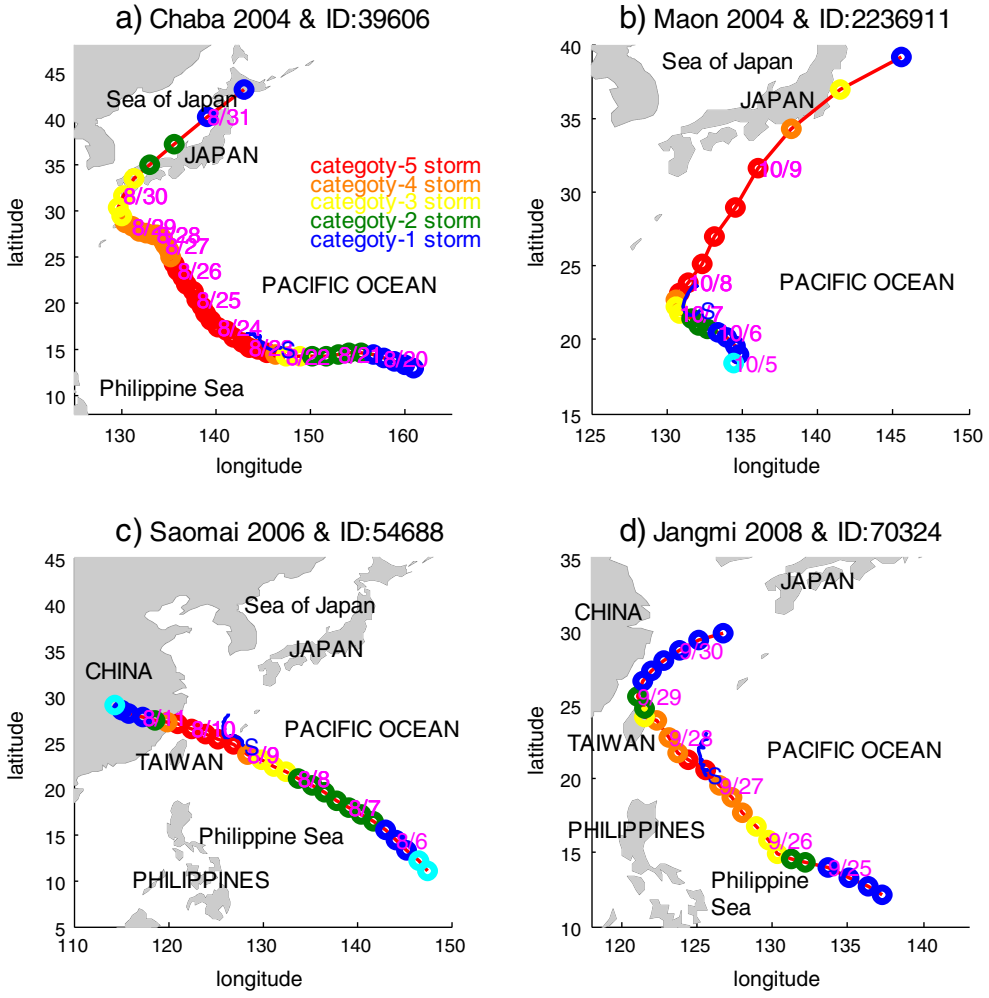


**Fig. 1.** Tracks of four super typhoons (red curve) [(a) Chaba, (b) Maon, (c) Saomai, (d) Jangmi] and four SVP drifters (blue curve) [(a) 39606, (b) 2236911, (c) 54688, (d) 70324] for the northwestern Pacific Ocean in (a) August 2004, (b) October 2004, (c) August 2006, and (d) September 2008 at 6 hour time interval with the storm's intensities by color circles.

increased (0.4, 0.7, 0.8, 1.1, and 1.7 m $s^{-1}$). Due to the slower $U_h$ and the curved storm track (Fig. 3b), the drifter moved towards the storm's center, and stayed at $D \sim R_{max}$ for the following 36 h (18:00 on 6 October–00:00 on 8 October). During that period, Maon rapidly intensified, and became a category-5 typhoon at 18:00 on 7 October. At that time, a maximum velocity of 2.6 m $s^{-1}$ was measured ($U_h = 2.9$ m $s^{-1}$, $D = 52$ km).

Saomai (2006) was a fast-moving storm. Its translation speeds were usually 6–9 m $s^{-1}$ (Fig. 6). As approaching rapidly to the drifter 54688 ($D = 287$, 108, and 74 km), it strengthened to a category-5 typhoon. But the observed current velocities increased slowly ($U_{obs} = 0.7$, 1.1, and 1.2 m $s^{-1}$), with a maximum velocity of 1.2 m $s^{-1}$ ($U_h = 8.1$ m $s^{-1}$, and $D = 74$ km).

Jangmi (2004) was also a fast-moving TC. At 12:00 on 26 September, Jangmi became a category-4 storm, and approached the drifter 70324 ($D = 484$ km, $U_h = 6.4$ m $s^{-1}$). The drifter-measured $U_{obs}$ was 0.6 m $s^{-1}$ (Fig. 7). When Jangmi reached category 5 intensity at 06:00 on 27 September, its translation speed $U_h$ decreased to 6.7 m $s^{-1}$; and $U_{obs}$ increased to 0.8 m $s^{-1}$ ($D = 88$ km). But, the drifter was in front of the storm center at that time (Direction = 25°). Six hours later, it was still a category-5 typhoon, and the translation speed $U_h$ increased slightly to 6.8 m $s^{-1}$. The drifter was on the right side of the storm center (Direction = 110°). A maximum velocity of 1.4 m $s^{-1}$ was measured ($D = 86$ km). Thus, besides the storm's intensity, the two parameters ($D$, $U_h$) are also important for causing high current speeds.

## 4. Dependence of observational current velocity ($U_{obs}$) on $U_h$

The maximum current velocities under Chaba, Maon, Saomai, and Jangmi were 2.1, 2.6, 1.2, and 1.4 m $s^{-1}$ (Figs. 4, 5, 6, and 7) when they were in category 5, with the distance $D = 52$–85 km, i.e., within 1–2 $R_{max}$ from the TC center [mean $R_{max} = 47$ km (Hsu and Yana, 1998)]. Although the four drifters were under comparable storm intensities with similar distances ($D$), different maximum current velocities (2.1, 2.6, 1.2, and 1.4 m $s^{-1}$) were observed. Note that the TC's translation speeds ($U_h$) were very different: 5.1, 2.9, 8.1, and 6.8 m $s^{-1}$, as the maximum velocities were observed.

Traditionally, the ocean OML currents during typhoon passage are mainly determined by the wind stress with a maximum current speed located to the right of the storm track at ~1–2$R_{max}$ (Brooks, 1983; Chang et al., 2013). Within this range the linear regression was conducted between $U_{obs}$ (unit: m $s^{-1}$) on the right side of the storm center (45° ≦ Direction ≦ 135°, see Table 3) and $U_h$ at $D \sim 1$–2 $R_{max}$ ($D = 38$–95 km, see Table 3),

$$U_{obs} = -0.256U_h + 3.24 \left(2.9 \text{ m s}^{-1} \leqq U_h \leqq 8.1 \text{ m s}^{-1}\right) \quad (1)$$

as shown in Fig. 8 (blue color "x" and lines) with a high correlation coefficient (−0.958). The p-value is 0.05 and 95% prediction interval was used. As the translation speeds of super typhoons are 3, 4, 5, 6, 7, and 8

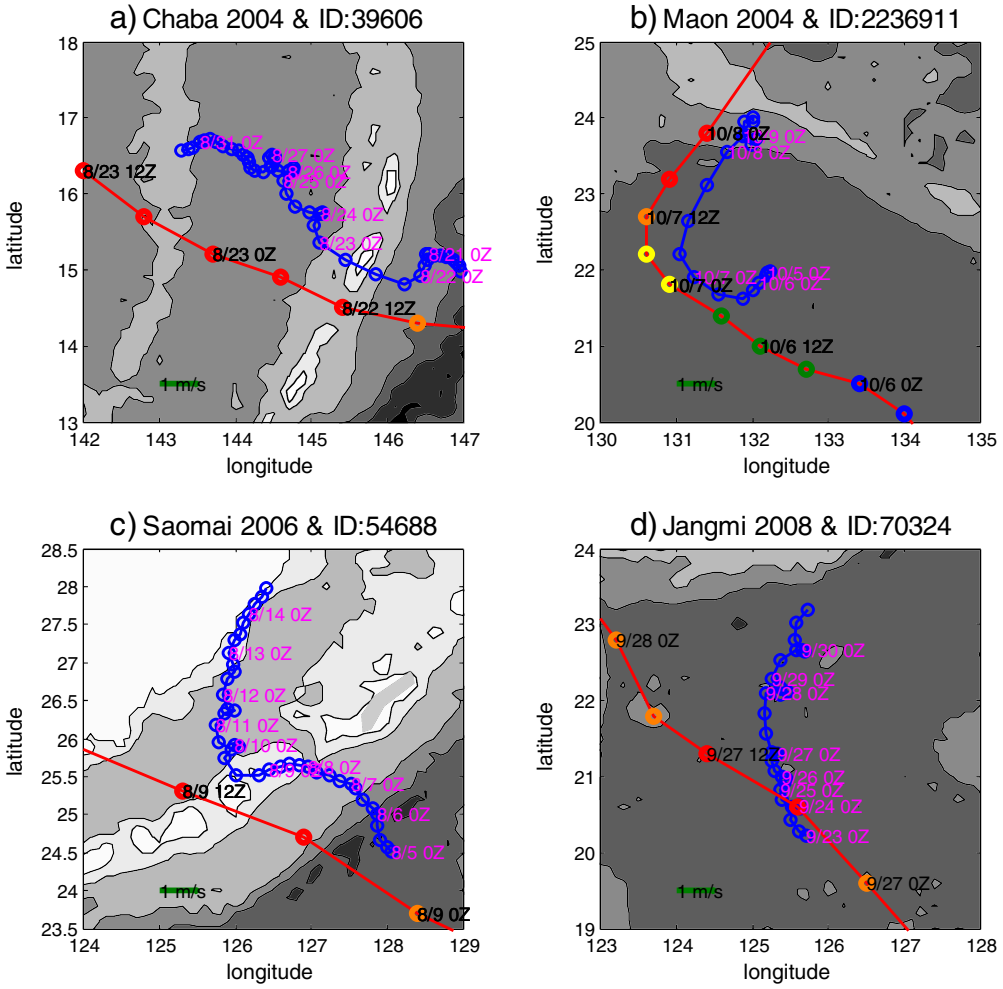


**Fig. 2.** Four storms' paths and four drifters' trajectories, both in 6-hourly interval.

m $s^{-1}$, the corresponding current velocities at ~1–2 $R_{max}$ are approximately 2.5 ± 0.6, 2.2 ± 0.6, 2.0 ± 0.5, 1.7 ± 0.5, 1.5 ± 0.6, and 1.2 ± 0.6 m $s^{-1}$. Figs. 4–7 show significant decrease of the OML velocity at several $R_{max}$ away from the TC track, especially 150 to 200 km (~3–4$R_{max}$) from the storm center.

Due to more sampling velocity data points were available in this study for each storm during the stage of very strong winds in larger range of $D$ ~ 0.5–3$R_{max}$ ($D$ = ~24–141 km), the linear regression was further conducted under category-5 storms between $U_{obs}$ (unit: m $s^{-1}$) on the right side of the storm center (30°≦Direction≦150°, see Table 3) and $U_h$ at $D$ = ~0.5–3$R_{max}$,

$$U_{obs} = -0.247U_h + 3.13 \left(2.9 \text{ m s}^{-1} \leqq U_h \leqq 8.7 \text{ m s}^{-1}\right) \quad (2)$$

as shown in Fig. 8 (red color circles and lines) with a high correlation coefficient (−0.932). The 95% prediction interval was also used. The dependence of $U_{obs}$ on $U_h$ under super typhoons is quite stable from the comparison between Eq. (1) and Eq. (2).

## 5. Dependence of the maximum velocity ($U_{max}$) on the TC's intensity (S)

Quantitative dependence of the maximum velocity ($U_{max}$) on the Saffir–Simpson hurricane scale ($S$) has not been established. Table 4 shows the qualitative relationship between $U_{max}$ and $S$. In order to construct a statistical relationship between mean $U_{max}$ (unit: m $s^{-1}$) inside $D$ ~ 3$R_{max}$ ($D$ < ~150 km) and the Saffir–Simpson hurricane scale ($S$) from a tropical storm to a category-5 super typhoon, the mean OML velocity data under all storms from the earlier studies (shown in Table 1) and from the SVP drifters under the four category-5 typhoons from this study are combined to get a linear regression equation using a 95% prediction interval,

$$U_{max} = 0.234S + 0.689 \ (0 \leqq S \leqq 5) \quad (3)$$

which shows a strong linear relationship with a high correlation coefficient (0.98) between $U_{max}$ and $S$ with one standard deviation as the error bars (Fig. 9).

Chang et al. (2012) used 11 years of wind and drifter data to show the relationship between the mean SVP drifter-measured ocean current speeds and the observed wind speeds of QuikSCAT with the error bars of one standard deviation for high wind speed of 20–50 m $s^{-1}$. The SVP drifter-measured ocean current velocities have errors of 0.3, 0.4, and 0.5 m $s^{-1}$ for 20, 35, and 47 m $s^{-1}$ winds, respectively. The results of Chang et al. (2012) were also plotted in Fig. 9 as the color blue. The mean velocity and error bars of one standard deviation in the study under S = 0, 1, 2 (red color) are consistent with the results of Chang et al. (2012).

Using 40 years of storm track data, Mei et al. (2012) suggested 5.4 m $s^{-1}$ as the mean $U_h$ for category-5 storms, and 4.5 m $s^{-1}$ for tropical storms. In order to construct general relationships between $U_{max}$ (unit: m $s^{-1}$) inside ~3$R_{max}$ and $S$ for slow- and fast-moving storms, we separated storms into "slow-moving" ($U_h$ = 2.0–4.0 m $s^{-1}$), "typically-

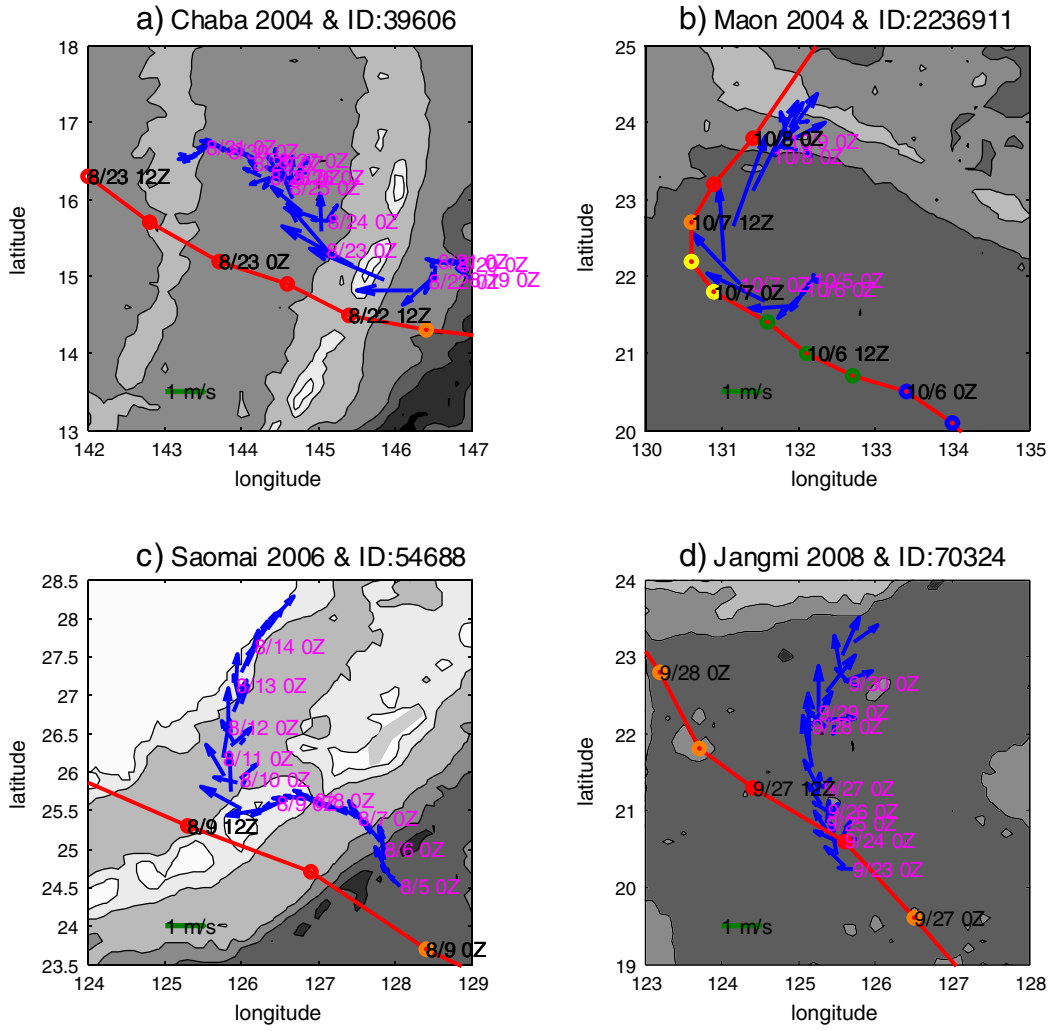


**Fig. 3.** Four storms' paths and observed current vectors, both in 6-hourly interval.

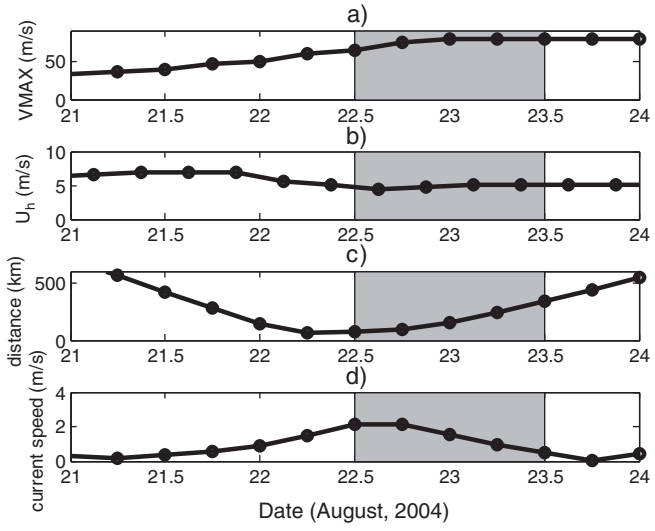


**Fig. 4.** Time evolution (6 hourly) of (a) storm's maximum sustained wind speed (VMAX), (b) storm's translation speed ($U_h$), (c) distances ($D$) between storm's center and drifter 39606 and (d) observed current speeds during Chaba. Shadings denote the duration during which the drifter was under a super typhoon and affected by the typhoon ($D < 400$ km).

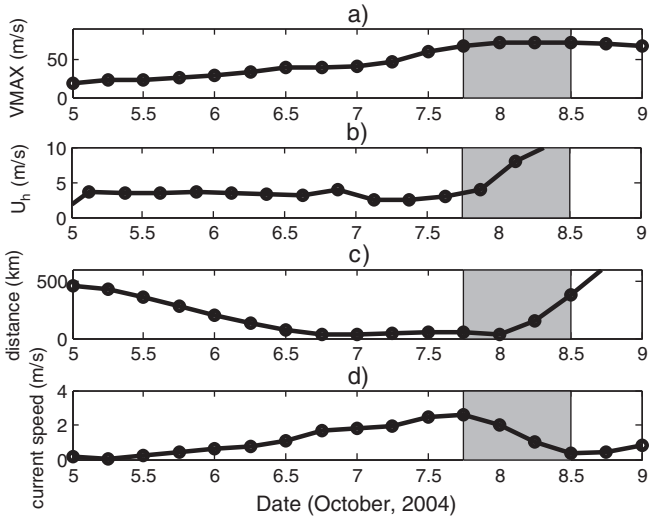


**Fig. 5.** Time evolution (6 hourly) of (a) storm's maximum sustained wind speed (VMAX), (b) storm's translation speed ($U_h$), (c) distances ($D$) between the storm's center and drifter 2236911 and (d) observed current speeds during Maon. Shadings denote the duration during which the drifter was under a super typhoon and affected by the typhoon ($D < 400$ km).

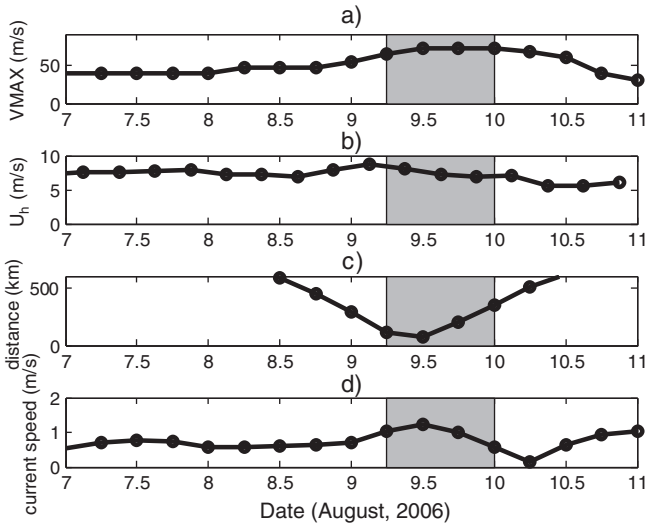


**Fig. 6.** Time evolution (6 hourly) of (a) Saomai's maximum sustained wind speed (VMAX), (b) storm's translation speed ($U_h$), (c) distances ($D$) between storm's center and drifter 54688 and (d) observed current speeds during Saomai. Shadings denote the duration during which the drifter was under a super typhoon and affected by the typhoon ($D < 400$ km).

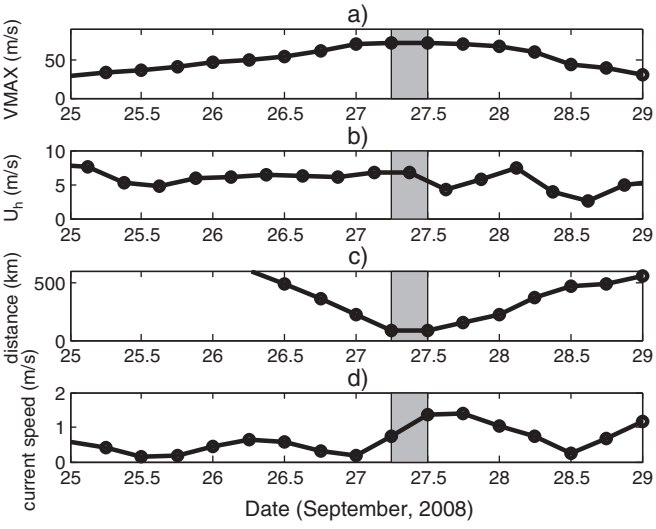


**Fig. 7.** Time evolution (6 hourly) of (a) Jangmi's maximum sustained wind speed (VMAX), (b) storm's translation speed ($U_h$), (c) distances ($D$) between storm's center and drifter 70324 and (d) observed current speeds during Jangmi. Shadings denote the duration during which the drifter was under a super typhoon and affected by the typhoon ($D < 400$ km).

moving" ($U_h$ = 4.0–6.0 m s$^{-1}$) and "fast-moving" ($U_h$ =6.0–8.0 m s$^{-1}$) categories. Two linear regressions,

$$U_{max} = 0.334S_{Slow} + 0.814 \ (0 \leqq S_{Slow} \leqq 5), \tag{4}$$

$$U_{max} = 0.141S_{fast} + 0.577 \left(0 \leqq S_{fast} \leqq 5\right), \tag{5}$$

are obtained with a 95% prediction interval (Fig. 10). Four maximum velocities under typical-moving storms fall in the region between the two regression lines. The $U_{max}$ under Ivan 2004 (Teague et al., 2007) had a larger current speed of 2.1 m s$^{-1}$, because the $U_{max}$ was observed at 6 m depth by an ADCP. The observed velocity of 2.1 m s$^{-1}$ at 6 m depth could contain a higher Stoke drift velocity. These general relationships between maximum OML velocity and all storms' intensity levels from observed data would also benefit modeling and simulation.

## 6. Current velocity scale ($U_s$)

The current velocity scale ($U_s$) (or called the expected current velocity) in the OML to a moving storm is estimated by Price (1983),

$$U_s = \frac{\tau_s R_{max}}{\rho_0 h U_h}, \tag{6}$$

where $\tau_s$ is the magnitude of the surface wind stress; $\rho_0$ is the characteristic density of seawater (~1025 kg m$^{-3}$); and $h$ is the OML depth, which is usually taken as 50 m in the northwestern Pacific during summer from the National Oceanographic Data Center (NODC) objectively analyzed monthly mean data (Chang et al., 2013). The climatological (summer) World Ocean Atlas (WOA) temperature profiles from NODC were used to show the OML depth at each grid point in the Gulf of Mexico, the North Atlantic, and the North Pacific in Fig. 11. The summer OML depths are about 50 m in the western equatorial Pacific and Atlantic. The summer OML depth in the Gulf of Mexico is closer to 40 m. In the previous study, Price et al. (1994) also used OML depths of 50 m and 60 m in the Gulf of Mexico to calculate $U_s$ during Hurricanes Gloria and Josephine. Thus, we use $h$ = 50 m to calculate $U_s$ in Eq. (6).

The wind stress ($\tau_s$) is given by

$$\tau_s = \rho_a C_D W^2 \tag{7}$$

where $\rho_a$ is the air density; $C_D$ is the drag coefficient; and $W$ is the wind speed at 10 m height. Typically, $\rho_a$ is about 1.22 kg m$^{-3}$ for the moist air (Zedler, 2009). Recent results indicated a saturation value of $C_D$ at the wind speed of 28–33 m s$^{-1}$ (Donelan et al., 2004; Jarosz et al., 2007; Powel et al., 2003). Three semi-empirical formulas from Powel et al. (2003), Black et al. (2007), and Jarosz et al. (2007) are used in this

**Table 3**
Observed ($U_{obs}$) and ageostrophic ($U_{ageo}$) current velocities under super typhoons with $D$ < 400 km.

| Name & ID | Time | Scale | $U_h$ (m s$^{-1}$) | $D$ (km) | Direction (degree) | $U_{obs}$ (m s$^{-1}$) | $U_{ageo}$ (m s$^{-1}$) |
|---|---|---|---|---|---|---|---|
| Chaba & 39606 | 1200 22 Aug | Category 5 | 5.1 | 69 | 120 | 2.1 | 1.9 |
| | 1800 22 Aug | Category 5 | 4.5 | 95 | 135 | 2.1 | 2.0 |
| | 0000 23 Aug | Category 5 | 4.7 | 152 | 150 | 1.6 | 1.5 |
| | 0600 23 Aug | Category 5 | 5.2 | 238 | * | 1.0 | 1.1 |
| | 1200 23 Aug | Category 5 | 5.0 | 338 | * | 0.5 | 0.7 |
| Maon & 2236911 | 1800 7 Oct | Category 5 | 2.9 | 52 | 60 | 2.6 | 2.5 |
| | 0000 8 Oct | Category 5 | 3.9 | 38 | 100 | 2.0 | 2.0 |
| | 0600 8 Oct | Category 5 | 7.9 | 153 | 150 | 1.0 | 1.1 |
| | 1200 8 Oct | Category 5 | 10.6 | 382 | * | 0.4 | 0.5 |
| Saomai & 54688 | 0600 9 Aug | Category 5 | 8.7 | 108 | 40 | 1.1 | 0.8 |
| | 1200 9 Aug | Category 5 | 8.1 | 74 | 135 | 1.2 | 1.2 |
| | 1800 9 Aug | Category 5 | 7.2 | 196 | * | 1.0 | 1.0 |
| | 0000 10 Aug | Category 5 | 7.0 | 351 | * | 0.6 | 0.6 |
| Jangmi & 70324 | 0600 27 Sep | Category 5 | 6.7 | 88 | 25 | 0.8 | 0.8 |
| | 1200 27 Sep | Category 5 | 6.8 | 85 | 110 | 1.4 | 1.4 |

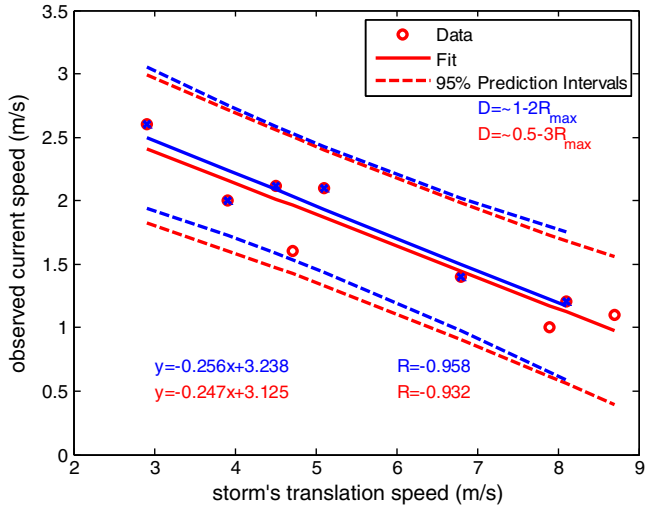


**Fig. 8.** Dependence of the observed current velocity ($U_{obs}$) on the storm's translation speed ($U_h$) under three category-5 storms at ~1–2$R_{max}$ (blue color) and ~0.5–3$R_{max}$ (red color).

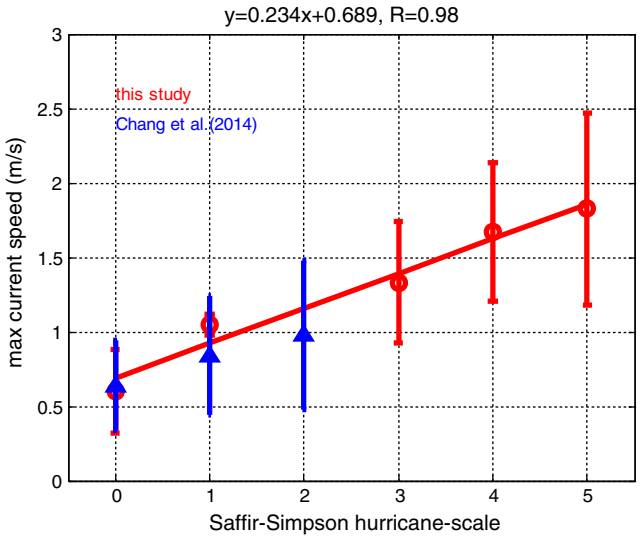


**Fig. 9.** Dependence of observed current speed on the Saffir–Simpson hurricane scale ($S$) with the error bars showing one standard deviation ($S = 0$: the tropical storm, $S = 1$: the category-1 storm, $S = 2$: the category-2 storm, …, etc.).

study to represent such dependence of $C_D$ on $W$ (Zedler et al., 2009). Thus, the estimated wind stress $\tau$ under category-5, -4, -3, -2, -1 storms and tropical storm can be calculated from the wind speeds of 70, 65, 55, 45, 40, and 30 m s$^{-1}$ (see Table 4). The estimated storm's $U_h$ was also listed in Table 4. The scaled current speeds ($U_s$), which were estimated from $C_D$ of Jarosz et al. (2007), are more similar to the observed $U_{max}$ (Table 4). Since the direct surface wind measurements are sparse under tropical cyclones, uncertainty exists in the estimate of maximum sustained wind speed (VMAX) and $R_{max}$.

The effects of OML depth, Stokes drift, and local background flow should also be addressed. The OML depth was taken as 40–50 m for the northwestern Pacific during summer in previous studies (Chang et al., 2013; de Boyer Montegut et al., 2004), however, it varies in time and space depending on the fluxes of momentum, heat, and moisture across the air–ocean interface, the gradient below the mixed layer, and upwelling (Chu, 1993; Chu et al., 1990; Chu and Garwood, 1991). Ardhuin et al. (2009) indicated that the surface wind-related Lagrangian velocity is the sum of the strongly sheared Stokes drift and a relatively uniform quasi-Eulerian current in the open ocean. The wave data in the four super typhoons are not available. The SVP drifter measurements are drogued to 15-m depth, which is still in a region of significant swell influence (Terray et al., 1996). The spatially asymmetric wave Stokes drift velocity imposed in the large-eddy simulation is generated by a spectral wave prediction model adapted to a category-4 hurricane (Frances 2004) moving at a speed of 5.5 m s$^{-1}$ (Sullivan et al., 2012). The largest Stokes drift at the water surface occurs in along-track component of approximately 0.5 m s$^{-1}$ on the right side of the storm track. The Stokes drift velocity decays with depth rapidly from the surface on a scale (i.e., the Stokes depth). The local background flow or vorticity can change the current structure and the frequency of the near-inertial

**Table 4**
Quantitative dependence of the maximum current velocity ($U_{max}$) on the Saffir–Simpson hurricane scale ($S$) under slow-moving ($U_h$ = 2.0–4.0 m s$^{-1}$), fast-moving ($U_h$ = 6.0–8.0 m s$^{-1}$), and all storms ($U_h$ ~ 4.9 m s$^{-1}$) (Chang et al., 2013) and comparison between the observed $U_{max}$ and the scaled wind-driven velocity $U_s$.

| Typhoon scale (Saffir–Simpson) | Storm's translation speed | Max current velocity, $U_{max}$ (m s$^{-1}$) | Wind-driven horizontal velocity, $U_s$ (m s$^{-1}$), [$C_D$ from Powel et al. (2003), Black et al. (2007), and Jarosz et al. (2007)] |
|---|---|---|---|
| Tropical storm (W = 30 m s$^{-1}$) | Slow-moving | 0.8 | 0.7, *0.5*, **0.8** |
| | All | 0.7 | 0.4, *0.3*, **0.5** |
| | Fast-moving | 0.6 | 0.3, *0.2*, **0.4** |
| Category-1 (W = 40 m s$^{-1}$) | Slow-moving | 1.2 | 1.1, *0.9*, **1.3** |
| | All | 0.9 | 0.7, *0.6*, **0.8** |
| | Fast-moving | 0.7 | 0.5, *0.4*, **0.6** |
| Category-2 (W = 45 m s$^{-1}$) | Slow-moving | 1.5 | 1.4, *1.1*, **1.4** |
| | All | 1.2 | 0.8, *0.7*, **0.8** |
| | Fast-moving | 0.9 | 0.6, *0.5*, **0.6** |
| Category-3 (W = 55 m s$^{-1}$) | Slow-moving | 1.8 | 1.7, *1.7*, **1.7** |
| | All | 1.4 | 1.0, *1.0*, **1.0** |
| | Fast-moving | 1.0 | 0.7, *0.7*, **0.7** |
| Category-4 (W = 65 m s$^{-1}$) | Slow-moving | 2.2 | 2.4, *2.4*, **2.4** |
| | All | 1.6 | 1.5, *1.5*, **1.5** |
| | Fast-moving | 1.1 | 1.0, *1.0*, **1.0** |
| Category-5 (W = 70 m s$^{-1}$) | Slow-moving | 2.5 | 2.7, *2.7*, **2.7** |
| | All | 1.9 | 1.7, *1.7*, **1.7** |
| | Fast-moving | 1.3 | 1.2, *1.2*, **1.2** |

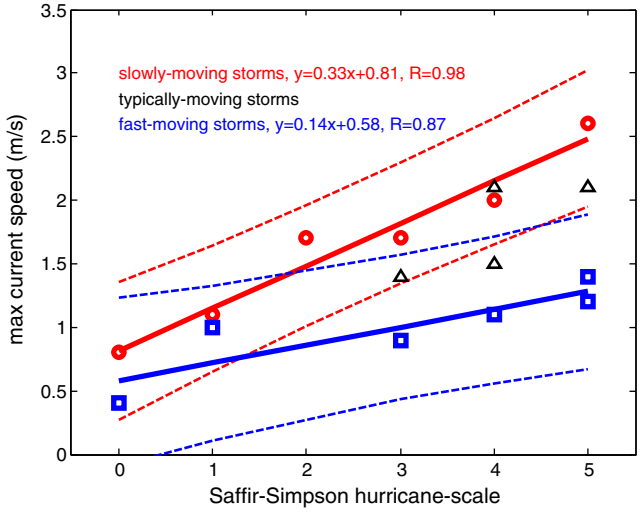


**Fig. 10.** Dependence of the maximum current velocity ($U_{max}$) on all storms' intensity levels ($S$) for slow-moving (red color, $U_h$ = 2.0–4.0 m s$^{-1}$), typical-moving (black color, $U_h$ = 4.0–6.0 m s$^{-1}$), and fast-moving storms (blue color, $U_h$ = 6.0–8.0 m s$^{-1}$) in earlier and this studies ($S = 0$: the tropical storm, $S = 1$: the category-1 storm, $S = 2$: the category-2 storm, …, etc.).

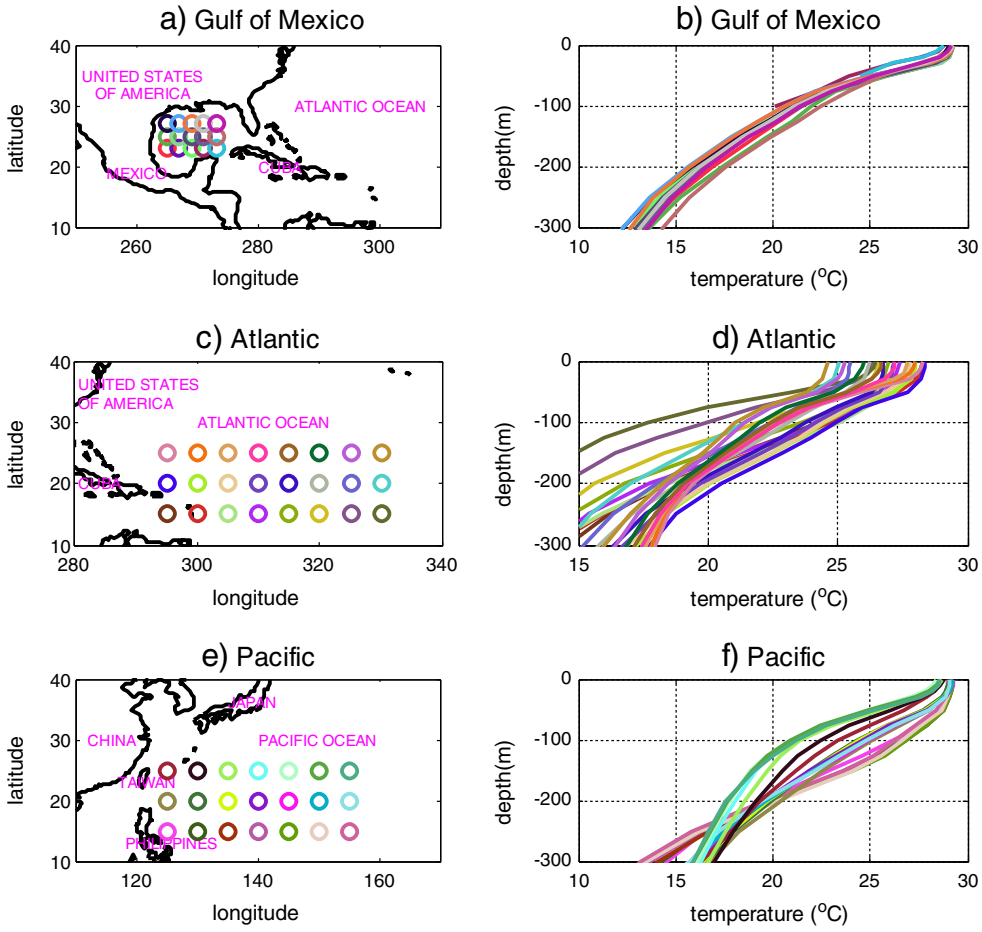


**Fig. 11.** Locations and temperature (°C) of NODC objectively analyzed mean data (a)–(b) in the Gulf of Mexico, (c)–(d) the northwestern Atlantic, and (e)–(f) the northwestern Pacific, during summer.

current. Background divergent flow will damp near-inertial motions (Gill, 1984; Jaimes and Shay, 2010).

## 7. Conclusions

This study characterizes the response of upper ocean velocity to the four super typhoons [Chaba (2004), Maon (2004), Saomai (2006), and Jangmi (2008)] in the northwestern Pacific from the analysis on the observed ocean current data from four SVP drifters and typhoon track data from JTWC. Strong OML currents occur to the right of the storm track under the four category-5 super typhoons from direct velocity measurements with maximum current velocities of 2.1, 2.6, 1.2, and 1.4 m $s^{-1}$ at ~1–2 $R_{max}$ ($D$ = 69, 52, 74, and 85 km). A unique and novel approach was provided to identify the strong near-surface currents in the wake of intense tropical cyclones. The general relationships between the observed current velocity and the storm's translation speed and between the maximum current velocities and the Saffir–Simpson hurricane scale are also provided. Our results are congruent with recent studies (Olabarrieta et al., 2012; Warner et al., 2010; Yablonsky and Ginis, 2009; Zambon et al., submitted for publication) and provide useful tool for model validation.

## Acknowledgments

This research was completed with grants from the Ministry of Science and Technology of Taiwan, Republic of China (MOST 102-2611-M-110-010-MY3) . Peter C. Chu was supported by the Naval Oceanographic Office (N6230612PO00123). We are grateful for the comments of two anonymous reviewers.

## References

Ardhuin, F., Marie, L., Rascle, N., Forget, P., Roland, A., 2009. Observation and estimation of lagrangian, Stokes, and Eulerian currents induced by wind and wave at the sea surface. J. Phys. Oceanogr. 39, 2820–2838.
Black, W.J., Dickey, T.D., 2008. Observations and analyses of upper ocean responses to tropical storm and hurricanes in the vicinity of Bermuda. J. Geophys. Res. 113, C08009. http://dx.doi.org/10.1029/2007JC004358.
Black, P., D'Asaro, E., Drennan, W., French, J., Niiler, P., Sanford, T., Terrill, E., Walsh, E., Zhang, J., 2007. Air–sea exchange in hurricanes: synthesis of observations from the coupled boundary layer air–sea transfer experiment. Bull. Am. Meteorol. Soc. 88 (3), 357–374.
Brink, K.H., 1989. Observations of the response of thermocline currents to a hurricane. J. Phys. Oceanogr. 19, 1017–1022.
Brooks, D.A., 1983. The wake of Hurricane Allen in the western Gulf of Mexico. J. Phys. Oceanogr. 13, 117–129.
Chang, S., Anthes, R., 1978. Numerical simulations of the ocean's nonlinear baroclinic response to translating hurricanes. J. Phys. Oceanogr. 8, 468–480.
Chang, Y.C., Tseng, R.S., Centurioni, L.R., 2010. Typhoon-induced strong surface flows in the Taiwan Strait and Pacific. J. Oceanogr. 66, 175–182.
Chang, Y.C., Chen, G.Y., Tseng, R.S., Centurioni, L.R., Chu, P.C., 2012. Observed near-surface currents under high wind speeds. J. Geophys. Res. 117, C11026. http://dx.doi.org/10.1029/2012JC007996.
Chang, Y.C., Chen, G.Y., Tseng, R.S., Centurioni, L.R., Chu, P.C., 2013. Observed near-surface flows under all tropical cyclone intensity levels using drifters in the northwestern Pacific. J. Geophys. Res. 118, 2367–2377.
Chu, P.C., 1993. Generation of low frequency unstable modes in a coupled equatorial troposphere and ocean mixed layer. J. Atmos. Sci. 50, 731–749.
Chu, P.C., Garwood Jr., R.W., 1991. On the two-phase thermodynamics of the coupled cloud-ocean mixed layer. J. Geophys. Res. 96, 3425–3436.
Chu, P.C., Garwood Jr., R.W., Muller, P., 1990. Unstable and damped modes in coupled ocean mixed layer and cloud models. J. Mar. Syst. 1, 1–11.

Chu, P.C., Veneziano, J.M., Fan, C.W., 2000. Response of the South China Sea to tropical cyclone Ernie 1996. J. Geophys. Res. 105, 13991–14009.
D'Asaro, E.A., Sanford, T.B., Niiler, P.P., Terrill, E.J., 2007. Cold wake of Hurricane Frances. Geophys. Res. Lett. 34, L15609. http://dx.doi.org/10.1029/2007GL030160.
de Boyer Montegut, C., Madec, G., Fischer, A.S., Lazar, A., Iudicone, D., 2004. Mixed layer depth over the global ocean: An examination of profile data and a profile-based climatology. J. Geophys. Res. 109, C12003. http://dx.doi.org/10.1029/2004JC002378.
Dickey, T., Frye, D., McNeil, J., Manov, D., Nelson, N., Sigurdson, D., Jannasch, H., Siegel, D., Michaels, T., Johnson, R., 1998. Upper-ocean temperature response to Hurricane Felix as measured by the Bermuda Testbed Mooring. Mon. Weather Rev. 126, 1195–1201.
Donelan, M.A., Haus, B.K., Reul, N., Plant, W., Stiassnie, M., Graber, H., Brown, O., Saltzman, E., 2004. On the limiting aerodynamic roughness of the ocean in very strong winds. Geophys. Res. Lett. 31, L18306. http://dx.doi.org/10.1029/2004GL019460.
Geisler, J.E., 1970. Linear theory of the response of a two-layer ocean to a moving hurricane. Geophys. Fluid Dyn. 1, 249–272.
Gill, A.E., 1984. On the behavior of internal waves in the wake of storms. J. Phys. Oceanogr. 14, 1129–1151.
Hansen, D., Poulain, P.M., 1996. Quality control and interpolations of WOCE-TOGA drifter data. J. Atmos. Ocean. Technol. 13, 900–909.
Hsu, S.A., Yana, Z., 1998. A note on the radius of maximum winds for hurricanes. J. Coastal Res. 12, 667–668.
Jacob, S.D., Shay, L.K., 2003. The role of oceanic mesoscale features on the tropical cyclone-induced mixed layer response: a case study. J. Phys. Oceanogr. 33, 649–676.
Jaimes, B., Shay, L.K., 2009. Mixed layer cooling in mesoscale oceanic eddies during hurricanes Katrina and Rita. Mon. Weather Rev. 137, 4188–4207.
Jaimes, B., Shay, L.K., 2010. Near-inertial wave wake of hurricanes Katrina and Rita over mesoscale oceanic eddies. J. Phys. Oceanogr. 40, 1320–1337.
Jarosz, E., Mitchell, D., Wang, D., Teague, W., 2007. Bottom-up determination of air–sea momentum exchange under a major tropical cyclone. Science 315, 1707–1709.
Kuo, Y.C., Chern, C.S., Wang, J., Tsai, Y.L., 2011. Numerical study of upper ocean response to a typhoon moving zonally across the Luzon Strait. Ocean Dyn. 61, 1783–1795.
Mei, W., Pasquero, C., Primeau, F., 2012. The effect of translation speed upon the intensity of tropical cyclones over the tropical ocean. Geophys. Res. Lett. 39, L07801. http://dx.doi.org/10.1029/2011GL050765.
Mitchell, D.A., Teague, W.J., Jarosz, E., Wang, D.W., 2005. Observed currents over the outer continental shelf during Hurricane Ivan. Geophys. Res. Lett. 32, L11610. http://dx.doi.org/10.1029/2005GL023014.
Niiler, P.P., 2001. The world ocean surface circulation. In: Siedler, G., Church, J., Gould, J. (Eds.), Ocean Circulation and Climate: Observing and Modeling the Global Ocean. Int. Geophys. Ser., 77. Academic Press, San Diego, Calif, pp. 193–204.
Niiler, P.P., Sybrandy, A.S., Bi, K., Poulain, P.M., Bitterman, D., 1995. Measurements of the water following capability of holey-sock and TRISTAR drifters. Deep-Sea Res. 42A, 1951–1964.
Olabarrieta, M., Warner, J.C., Armstrong, B., Zambon, J.B., He, R., 2012. Ocean–atmosphere dynamics during Hurricane Ida and Nor'Ida: an application of the coupled ocean–atmosphere–wave–sediment transport (COAWST) modeling system. Ocean Model. 43–44, 112–137. http://dx.doi.org/10.1016/j.ocemod.2011.12.008.
Powel, M., Vickery, P., Reinhold, T., 2003. Reduced drag coefficients for high wind speeds in tropical cyclones. Nature 422, 279–283.
Price, J.F., 1981. Upper ocean response to a hurricane. J. Phys. Oceanogr. 11, 153–175.
Price, J.F., 1983. Internal wave wake of a moving storm. Part I: scales, energy budget and observations. J. Phys. Oceanogr. 13, 949–965.
Price, J.F., Sanford, T.B., Forristall, G.Z., 1994. Forced stage response to a moving hurricane. J. Phys. Oceanogr. 24, 233–260.
Sanford, T.B., Black, P.G., Haustein, J.R., Feeney, J.W., Forristall, G.Z., Price, J.F., 1987. Ocean response to a hurricane. Part I: observations. J. Phys. Oceanogr. 17, 2065–2083.
Sanford, T.B., Price, J.F., Girton, J.B., 2011. Upper-ocean response to hurricane Frances (2004) observed by profiling EM-APEX floats. J. Phys. Oceanogr. 41, 1041–1056.
Shay, L.K., Elsberry, R.L., 1987. Near-inertial ocean current response to Hurricane Frederic. J. Phys. Oceanogr. 17, 1249–1269.
Shay, L.K., Uhlhorn, E.W., 2008. Loop current response to Hurricanes Isidore and Lili. Mon. Weather Rev. 137, 3248–3274. http://dx.doi.org/10.1175/2008MWR2169.
Shay, L.K., Black, P.G, Mariano, A.J., Hawkins, J.D., Elsberry, R.L., 1992. Upper ocean response to Hurricane Gilbert. J. Geophys. Res. 97, 20227–20248.
Sullivan, P.P., Romero, L., McWilliams, J.C., Melville, W.K., 2012. Transient evolution of Langmuir turbulence in ocean boundary layers driven by hurricane winds and waves. J. Phys. Oceanogr. 42, 1959–1980.
Teague, W.J., Jarosz, E., Wang, D.W., Mitchell, D.A., 2007. Observed oceanic response over the upper continental slope and outer shelf during Hurricane Ivan. J. Phys. Oceanogr. 37, 2181–2206.
Terray, E.A., Donelan, M.A., Agrawal, Y.C., Drennan, W.M., Kahma, K.K., Williams, A.J., Hwang, P.A., Kitaigorodskii, S.A., 1996. Estimates of kinetic energy dissipation under breaking waves. J. Phys. Oceanogr. 26, 792–807.
Tsai, Y., Chern, C.S., Wang, J., 2008. Typhoon induced upper ocean cooling off northeastern Taiwan. Geophys. Res. Lett. 35, L14605. http://dx.doi.org/10.1029/2008GL034368.
Warner, J.C., Armstrong, B., He, R., Zambon, J.B., 2010. Development of a coupled ocean–atmosphere–wave–sediment transport (COAWST) modeling system. Ocean Model. 35, 230–244.
Wu, C.-R., Chang, Y.-L., Oey, L.-Y., Chang, C.-W.J., Hsin, Y.-C., 2008. Air–sea interaction between Tropical Cyclone Nari and Kuroshio. Geophys. Res. Lett. 35, L12605. http://dx.doi.org/10.1029/2008GL033942.
Yablonsky, R.M., Ginis, I., 2009. Limitation of one-dimensional ocean models for coupled hurricane-ocean model forecasts. Mon. Weather Rev. 137, 4410–4419. http://dx.doi.org/10.1175/2009MWR2863.1.
Zambon, J.B., He, R., Warner, J.C., 2014. Investigation of Hurricane Ivan using the Coupled Ocean–Atmosphere–Wave–Sediment Transport (COAWST) Model. Ocean Dyn. 1–48 (submitted for publication).
Zedler, S.E., 2009. Simulations of the ocean response to a hurricane: nonlinear processes. J. Phys. Oceanogr. 39, 2618–2634.
Zedler, S.E., Niiler, P.P., Stammer, D., Terrill, E., Morzel, J., 2009. Ocean's response to Hurricane Frances and its implications for drag coefficient parameterization at high wind speeds. J. Geophys. Res. 114, C04016. http://dx.doi.org/10.1029/2008JC005205.